Bounding the Power Rate Function of Wireless Ad hoc Networks

Yunnan Wu*, Qian Zhang†, Wenwu Zhu†, Sun-Yuan Kung*.
*Dept. of Electrical Engineering, Princeton University. {yunnanwu, kung}@princeton.edu
†Microsoft Research, Asia, Beijing, P. R. China. {qianz, wwzhu}@microsoft.com

***Abstract*— Given a wireless ad hoc network and an end-to-end traffic pattern, the *power rate function* refers to the minimum total power required to support different throughput under a simplified layered model of wireless networks. A critical notion of the layered model is the *supported (realizable) capacity graphs*, which describe possible bit-rate provisions on the links by the physical and link layers. Under the layered model, the problem of finding the power rate function can be transformed into finding the minimum-power supported capacity graph that can provide a given throughput.**

We introduce a *usage conflict graph* to represent the conflicts among different uses of the wireless medium. Testing the realizability of a given capacity graph can be transformed into finding the (vertex) chromatic number, i.e., the minimum number of colors required in a proper vertex-coloring, of the associated usage conflict graph. Based on an upper bound of the chromatic number, we propose a linear program that outputs an upper bound of the power rate function. A lower bound of the chromatic number is the clique number. We propose a systematic way of identifying cliques based on a geometric analysis of the space sharing among active links. This leads to another linear program, which yields a lower bound of the power rate function. We further apply greedy vertex-coloring to fine tune the bounds. Simulations results demonstrate that the obtained bounds are tight in the low power and low rate regime.

I. Introduction

Throughput and energy efficiency are two important performance metrics for wireless ad hoc networks, each of which has been studied extensively in the literature [1]–[6]. Whereas one or the other may be more critical in certain wireless network, these two considerations do closely affect each other. A brief explanation is as follows. Consider multiple unicast sessions in a wireless network. For the sake of energy efficiency, each session would prefer the path along which the energy consumption is the minimum. However, if each session only routes packets along its individual minimum energy path, bottlenecks may be created, which would subsequently constrain the overall throughput. Higher throughput may be achieved by arranging some sessions to adopt routes with sub-optimal energy efficiency.

The subject of this paper is the tradeoff between throughput and energy efficiency for a given wireless network with a given end-to-end traffic pattern. Among others, characterizing such tradeoff can facilitate evaluating the efficiency of different network structures. Finding the optimal tradeoffs between throughput and energy efficiency essentially turns into addressing how the operational characteristics of a wireless network should be varied by coordinating the degrees of freedoms (e.g., routing, scheduling, power allocation, beam patterns) differently, as the offered traffic load changes.

Some recent works that investigate such tradeoff are as follows. Previous work [7] by Bhatia and Kodialam considered minimizing the total power consumed in providing different rates for a single unicast session. They formulated the problem as a nonlinear optimization. Previous work [8] by Cruz and Santhanam considered minimizing the total power consumed in providing different rates for multiple unicast sessions. Their formulation is also a nonlinear optimization. Previous work [9] by Wu et al considered minimizing the total power consumed in providing different rates for multiple multicast sessions. They proposed an iterative optimization that alternates between a linear optimization and a heuristic algorithm.

While very different modelling assumptions have been adopted in [7]–[9], these previous works used similar curves to quantitatively represent the tradeoff between throughput and energy efficiency. Based on these, we use the name *power rate function* to refer to the minimum total power required to support different end-to-end throughput for a given wireless network with a given traffic pattern, under a simplified layered model of wireless networks.

Note that the "minimum" investigated in this paper is certainly not the fundamental limit in network information theory, where lots of problems remain open. For example, the information theoretic capacity region for a simple network with a source, a relay, and a destination,

remains unknown. Instead, we adopt a simplified layered model of wireless networks. The basic assumptions of the layered model are as follows. The physical and link layers of the wireless network provide communication resources in the form of a collection of "lossless bit-pipes", each capable of transferring information between (neighboring) nodes at a certain rate. Given a collection of lossless bit-pipes, information can be routed from the sources to the destinations at certain rates in the network layer. Such a simplified model is certainly sub-optimal from an information theoretic perspective. Nonetheless, its simplicity facilitates the analysis and enables some engineering insights to be obtained. In fact, these assumptions have been implicitly or explicitly made in many recent works, such as [1]–[3], [7]–[9].

To explain the layered model in more details, we adopt the terminologies and notations in [9]. A collection of lossless bit-pipes mentioned earlier is called a *capacity graph* in [9]. A *capacity graph* can be represented as a tuple $G = (V, E, c)$ where V and E are the set of vertices and edges respectively and there is a positive edge capacity $c(vw)$ associated with each directed edge vw. At the physical layer, the network operates in many different *physical states*, each corresponding to an arrangement of concurrent transmissions among neighbors. Each physical state corresponds to an *elementary capacity graph*. At the MAC layer, by timesharing different physical states, convex combinations of the elementary capacity graphs can be achieved, hence presenting to the upper layers a set of supported *composite capacity graphs*.

Each supported capacity graph G provides certain communication rate $R(G)$ and has an associated power consumption $P(G)$, corresponding to the two axes under investigation. The problem of finding the power rate function, in the end, turns into one where the *optimal* supported capacity graph, associated with each traffic rate, is the target. However, computational difficulties can arise when searching over the entire set of supported capacity graphs, since the number of elementary capacity graphs to be considered can grow exponentially in the number of nodes.

In this work, we present a sufficient condition under which a capacity graph can be decomposed into a convex combination of elementary capacity graphs. We also present a necessary condition based on the fact each link exclusively occupies certain spatial region. These conditions can be expressed as linear constraints. The sufficient condition identifies a subset of supported capacity graphs and the necessary condition identifies a superset of the set of capacity graphs. By optimizing the multi-commodity flow assignment over the subset (resp. the superset) with power minimization as the objective, we obtain a linear program that yields an upper-bound (resp. a lower bound) to the power rate function.

The solution to a linear program mentioned above transforms the end-to-end traffic demand into a particular capacity graph that need to be supported. For each resulting capacity graph, we propose to apply a greedy coloring procedure to scale the obtained power rate pair and hence improve the bounds.

II. Preliminaries: Modelling Assumptions

A. Physical Layer Model

Let V_0 denote the set of nodes in a wireless network, which are labelled $1, 2, \ldots, |V_0|$. Let X_i denote the location of node i. Assume there is a fixed transmission power $p_{ij} = \kappa |X_i - X_j|^\beta$ associated with each link ij, where κ and β are two positive constants. Further assume there is a limit p_{max} on the maximum transmission power that can be used. Thus, a wireless link ij is regarded as feasible, or node i can directly transmit to node j, if and only if $p_{ij} \leq p_{max}$. In other words, the *connectivity graph* C, i.e., the graph of all possible links, has vertex set V_0 and edge set $E_C = \{ij \,|p_{ij} \leq p_{max}\}$.

We adopt the *conflict graph* defined by Jain et al [3] as the interference model. The vertices in the conflict graph I correspond to links in the connectivity graph. The edges in I represent conflict relationships among links in E_C.

Definition 1 (Conflict Graph [3]):
The *conflict graph* is an undirected graph I with $V(I) = E_C$. There is an undirected edge between vertices ij and kl if the links ij and kl conflicts and thus cannot be concurrently active.

More specifically, here link ij and kl are allowed to be concurrently active if and only if

$$|X_k - X_j| \geq (1 + \nu)|X_k - X_l|, \tag{1}$$
$$|X_i - X_l| \geq (1 + \nu)|X_i - X_j|, \tag{2}$$

where ν is a positive constant. Note that conditions (1) and (2) implies that each node can only transmit to or receive from at most one other node at any time. With some simple geometric arguments, the following Lemma 1 can be established.

Lemma 1: Under the physical layer model described

above, if link ij and kl can be concurrently active, then

$$|X_j - X_l| \geq \frac{\nu}{2}\left(|X_i - X_j| + |X_k - X_l|\right), \quad (3)$$

$$|X_k - X_i| \geq \frac{\nu}{2}\left(|X_i - X_j| + |X_k - X_l|\right), \quad (4)$$

$$|X_k - X_j| \geq \frac{\nu}{2}\left(|X_i - X_j| + |X_k - X_l|\right), \quad (5)$$

$$|X_i - X_l| \geq \frac{\nu}{2}\left(|X_i - X_j| + |X_k - X_l|\right). \quad (6)$$

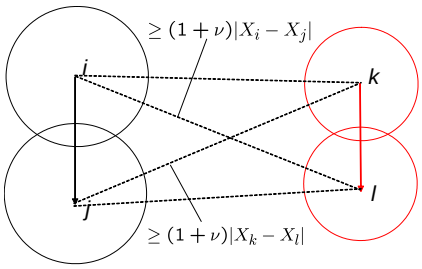

Fig. 1. Exclusive share of space.

Introduce

$$\Omega(ij) \equiv \left\{ X \,\middle|\, \min\{|X - X_i|,\ |X - X_j|\} \leq \frac{\nu}{2}|X_i - X_j| \right\}$$

which refers to the spatial region comprising points falling into one of the two circles centered at X_i and X_j with radius $\frac{\nu}{2}|X_i - X_j|$. According to Lemma 1, if link ij and kl can be concurrently active, then $\Omega(ij) \cap \Omega(kl) = \emptyset$, as illustrated in Figure 1. Thus, when a wireless link ij is active, it exclusively occupies the spatial region $\Omega(ij)$.

This exclusive sharing of space constrains the maximum achievable throughput. In [1], with a different interference model, Gupta and Kumar showed that a wireless link exclusively shares a disk centered at the receiver. The observation was used to establish a tight upper bound of the asymptotic scaling rate of transport capacity.

Summary: A set of wireless links A is allowed to be concurrently active if no conflict exists between any two links in A. Under our modeling assumptions, a physical state of interest can be characterized entirely by the set of wireless links that are active. For a given physical state with active links $A \subseteq E_C$, the associated elementary capacity graph G_A is $(V_0, A, \mathbf{1})$; that is, G_A has a set of edges $A \subseteq E_C$, each assigned unit capacity. The power consumption of G_A is then

$$p(G_A) = \sum_{ij \in A} p_{ij}. \quad (7)$$

B. Structure of Supported Capacity Graphs [9]

By timesharing among different physical states, it is possible to achieve any convex combination of the elementary capacity graphs. That is, if λ_k is the relative share of time for the elementary capacity graph $G_k = (V_k, E_k, c_k)$, then it is possible to achieve on average the capacity graph $G = \sum_k \lambda_k G_k \equiv (\cup_k V_k, \cup_k E_k, \sum_k \lambda_k c_k)$. The capacity graphs resulting from timesharing the elementary capacity graphs will be referred to as *composite capacity graphs*; conversely, the composite capacity graphs are said to be *decomposable* into elementary capacity graphs as a realization through timesharing. Hence, a distinguishing feature of wireless networks is the characterization of supported capacity graphs as a convex combination of elementary capacity graphs. This can be stated mathematically as

$$\mathcal{G}_0 = \left\{ G \,\middle|\, G = \sum_k \lambda_k G_k,\ \sum_k \lambda_k \leq 1,\ \lambda_k \geq 0\ \forall k, G_k \in \mathcal{B}_0 \right\},$$

where $\mathcal{G}_0$ is the entire set of capacity graphs supported/spanned by the set of all feasible elementary capacity graphs $\mathcal{B}_0$. For later use, we introduce the following definition.

Definition 2: A capacity graph $G = (V, E, c)$ is said to be *supported* or *realizable* if $G \in \mathcal{G}_0$ or equivalently, there exists a set of elementary capacity graphs $\{G_k\} \subseteq \mathcal{B}_0$ and a set of timesharing coefficients $\{\lambda_k\}$ such that

$$G = \sum_k \lambda_k G_k, \quad \sum_k \lambda_k \leq 1. \quad (8)$$

The power consumption of a composite capacity graph $G = \sum_k \lambda_k G_k$ is

$$P\left(\sum_k \lambda_k G_k\right) = \sum_k \lambda_k p(G_k). \quad (9)$$

Since the power associated with an elementary capacity graph G_k is simply the sum of the power of the associated active links, the power consumption of a supported capacity graph $G = (V_0, E_C, c)$ can be immediately obtained as

$$P(G) = \sum_{vw \in E_C} c(vw) p_{vw}, \quad (10)$$

although the decomposition into convex combinations of elementary capacity graphs may not be unique.

C. Traffic Pattern

We represent the end-to-end communication demands as a collection of unicast sessions in the form $\mathcal{S}_m \equiv \langle s^m, t^m, \alpha^m R \rangle$, $s^m \in V_0$, $t^m \in V_0$, $\alpha^m > 0$, $m = 1, \ldots, M$. In unicast session $\mathcal{S}_m$, a sender s^m transmits information to a receiver t^m at rate $\alpha^m R$ (bps). As a modeling simplification, we adopt the traffic scaling factor R as a scalar measure of rate, since the power rate tradeoff, rather than the throughput tradeoff among users, is our current focus.

D. Multi-commodity Flow on a Given Capacity Graph

Routing the traffic demands $\{\mathcal{S}_m\}$ on a given capacity graph $G = (V, E, c)$ amounts to the well-known multi-commodity flow problem in graph theory. Traffic demands $\{\mathcal{S}_m\}$ can be accommodated by a multi-commodity flow assignment if and only if the following system of linear constraints has a feasible solution

$$f^m(vw) \geq 0, \quad \forall vw \in E, m = 1, \ldots, M \tag{11}$$

$$\sum_{m=1}^{M} f^m(vw) \leq c(vw), \quad \forall vw \in E,\ m = 1, \ldots, M \tag{12}$$

$$\sum_{w \in V: vw \in E} f^m(vw) - \sum_{w \in V: wv \in E} f^m(wv) = 0, \quad \forall v \in V \backslash \{s^m, t^m\},\ m = 1, \ldots, M \tag{13}$$

$$\sum_{w \in V: s^m w \in E} f^m(s^m w) - \sum_{w \in V: w s^m \in E} f^m(w s^m) = \alpha^m R, \quad m = 1, \ldots, M. \tag{14}$$

The maximum achievable rate on a given capacity graph G, $R(G)$, can be found by maximizing rate R subject to (11)-(14).

III. The Power Rate Function

Definition 3 (Achievable Power Rate Pair): A power rate pair (P, R) is said to be *achievable* if there exists a supported capacity graph G, which can accommodate rate R and has a power consumption $P(G) \leq P$.

Definition 4 (Power Rate Function): The power rate function $P(R)$ for a wireless network is the minimum of all power values P such that (P, R) is achievable for a given rate R.

Theorem 1: The power rate function $P(R)$ is nondecreasing and convex.

Proof: If (P_1, R_1) and (P_2, R_2) are achievable, then by timesharing, power rate pair $(\lambda_1 P_1 + \lambda_2 P_2, \lambda_1 R_1 + \lambda_2 R_2)$ is achievable, $\forall \lambda_1 \geq 0, \lambda_2 \geq 0$ and $\lambda_1 + \lambda_2 \leq 1$.

By setting $(P_2, R_2) = (0, 0)$, we can establish that $P(R)$ is nondecreasing. ∎

For an achievable power rate pair (P, R), the ratio P/R is the energy-per-bit, which can be used as a quantitative measure of energy efficiency. Introduce

$$E_b^{min} \equiv \inf_R \frac{P(R)}{R}. \tag{15}$$

The following Theorem 2 shows that the minimum energy-per-bit E_b^{min} is achievable and can be found by a linear program. This corresponds to the first linear segment of $P(R)$ starting from a rate of zero, as illustrated in Figure 3.

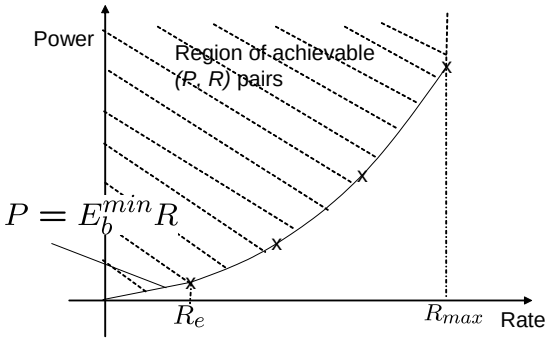

Fig. 3. The power rate function. The shaded region represents the set of achievable power rate pairs. The power rate function is the boundary of the achievable region and is nondecreasing and convex. Under the physical layer model of this paper, the power rate function is linear up to certain rate R_e with the slope being the minimum energy-per-bit E_b^{min}. R_{max} is defined as the maximum rate beyond which no higher rate can be supported regardless of the power consumption.

Theorem 2: The power rate function $P(R)$ is linear up to certain rate R_e with the slope being the minimum energy-per-bit, i.e.,

$$P(R) = E_b^{min} R, \quad R < R_e. \tag{16}$$

Proof: Let $G = (V_0, E_C, c)$ denote the capacity graph in the solution of the linear program in Figure 2. Thus, G achieves a rate $R(G) = 1$ at a power $P(G)$. There exists a scaling factor $\epsilon > 0$ such that $\epsilon G \in \mathcal{G}_0$ and the energy-per-bit is the same as G, i.e., $P(\epsilon G)/R(\epsilon G) = P(G)$.

We prove $P(G) = E_b^{min}$ by contradiction. Suppose instead there is a capacity graph $G^* \in \mathcal{G}_0$ such that

$$\frac{P(G^*)}{R(G^*)} < P(G). \tag{17}$$

Then $\frac{1}{R(G^*)} G^*$ would satisfy all the constraints in Figure 2, yet achieving a smaller power. This leads to a contradiction. ∎

IV. Realizability of a Given Capacity Graph

In this section, we ask the following question: "is a given capacity graph $G = (V_0, E_C, c)$ realizable as a convex combination of feasible elementary capacity graphs?"

A. Background: Vertex Coloring

The *neighborhood* of v in an undirected graph U is:

$$N(v) = \{w \in V : vw \in E(U)\} \tag{23}$$

The *degree* of a vertex v in U is $d(v) = |N(v)|$. The maximum degree of a graph U is

$$\Delta(U) = \max_{v \in U} d(v). \tag{24}$$

$$\min \sum_{vw \in E_C} c(vw) p_{vw} \quad \text{subject to:} \tag{18}$$

$$f^m(vw) \geq 0, \quad \forall vw \in E_C,\ m = 1, \ldots, M \tag{19}$$

$$\sum_{m=1}^{M} f^m(vw) \leq c(vw), \quad \forall vw \in E_C, \tag{20}$$

$$\sum_{w \in V_0 : vw \in E} f^m(vw) - \sum_{w \in V_0 : wv \in E} f^m(wv) = 0, \quad \forall v \in V_0 \backslash \{s^m, t^m\},\ m = 1, \ldots, M \tag{21}$$

$$\sum_{w \in V_0 : s^m w \in E} f^m(s^m w) - \sum_{w \in V : w s^m \in E} f^m(w s^m) = \alpha^m, \quad m = 1, \ldots, M \tag{22}$$

Fig. 2. A linear program which computes E_b^{min}.

A *proper vertex coloring* of an undirected graph U is an assignment of colors (or integer labels), one for each vertex of U, such that no two adjacent vertices receive the same color. The *(vertex) chromatic number*, $\chi(U)$, of an undirected graph U is defined as the minimum number of colors required in a proper vertex coloring.

A *clique* refers to a subset of vertices that induces a complete sub-graph. The *clique number* $\omega(U)$ of a graph U is the maximum number of vertices among the complete subgraphs of U.

Theorem 3 (See, e.g., [10]):

$$\omega(U) \leq \chi(U) \leq \Delta(U) + 1. \tag{25}$$

The lower bound $\omega(U)$ holds because the vertices in a clique of U must receive different colors in a proper coloring. The upper bound can be established by a greedy coloring algorithm. First, assign a fixed order to the vertices, say $v_1, \ldots, v_n$, $n = |V(U)|$. Then, visit the vertices in turn and assign each vertex v_i the first available color, i.e., the smallest color label that has not been used to color any neighbor of v_i. Thus $\Delta(U) + 1$ colors is sufficient with any order.

The following heuristic coloring order can be found in [11] and [12]: choose the last vertex v_n to be the one with the minimum degree in U; then choose v_{n-1} to be the one with the minimum degree in $U - v_n$; and so on.

B. Sufficient Condition for Realizability

Let a capacity graph $G = (V_0, E_C, c)$ represent the rates that need to be provided on the wireless links. We begin by illustrating the basic idea via Figure 4.

Assume the wireless network operates in a synchronous time-slotted mode and a single use of a wireless link takes one fixed time slot. In Figure 4, suppose link vw needs to be used twice and link pq needs to be used three times and etc. The conflict graph I describes conflicts among links and hence the rules of allowed coexistence in a time slot. We construct a *usage conflict graph* U, as illustrated on the right of Figure 4. Introduce two vertices vw_1, vw_2 to represent the uses, or *instances*, of link vw and three vertices pq_1, pq_2, pq_3 to represent the instances of link pq. Conflicts exist between link vw and pq; hence in U, each instance vw_i has edges with all instances of pq, pq_1, pq_2, and pq_3. Conflicts also exist between different instances of the same link vw; hence an edge is drawn between vw_1 and vw_2. A proper vertex coloring corresponds to a scheduling of links into time slots such that the scheduled links in any time slot can coexist without any conflict. The chromatic number $\chi(U)$ is then the minimum number of time slots required for conflict-free scheduling. Since there exists a certain conflict-free schedule where link vw is used twice and link pq is used three times over a period of $\chi(U)$ slots, rates $c(vw) = \frac{2}{\chi(U)}$, $c(pq) = \frac{3}{\chi(U)}$, can be supported on the two links.

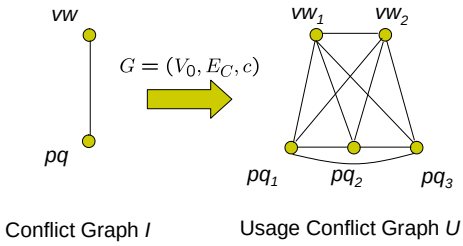

Fig. 4. Illustration of a usage conflict graph.

We can generalize from the explanation above and observe that the realizability of a capacity graph is equivalent to the existence of a conflict-free schedule of requested uses(instances) of the links over a long period,

which can be further linked with a proper vertex coloring of the usage conflict graph U. This observation is key to the following Theorem 4.

Theorem 4 (Sufficient Condition for Realizability): Under the model described in Section II, a given capacity graph $G = (V_0, E_C, c)$ is realizable if

$$c(vw) + \sum_{pq:\ pq \in N(vw)} c(pq) \leq 1 \quad \forall vw \in E_C. \tag{26}$$

Proof: Multiply both sides of (26) by a (large enough) integer number Q

$$Q\left[c(vw) + \sum_{pq:\ pq \in N(vw)} c(pq)\right] \leq Q \quad \forall vw \in E_C.$$

Without essential loss of generality, we can assume $Qc(vw)$, $\forall vw \in E_C$ are all integers. Construct a usage conflict graph U as follows. Corresponding to each vertex vw of I, we introduce $q = Qc(vw)$ vertices, vw_1, ..., vw_q in U. Fully connect these q edges in U, to reflect conflicts among uses of a same link. If $vw \in N(pq)$, then we put an edge between vw_i and pq_j, $\forall i, j$. The degree of a vertex vw_i in U is

$$d(vw_i) = Qc(vw) + \sum_{pq:\ pq \in N(vw)} Qc(pq) - 1. \tag{27}$$

Hence the maximum degree of U is

$$\begin{aligned}\Delta(U) &= \max_{vw \in E_C} Q\left[c(vw) + \sum_{pq:\ pq \in N(vw)} c(pq)\right] - 1 \\ &\leq Q - 1.\end{aligned}$$

According to Theorem 3,

$$\chi(U) \leq \Delta(U) + 1 \leq Q. \tag{28}$$

Thus, in Q time slots, each link vw can be used $Qc(vw)$ times, resulting in rates $\{c(vw)\}$ being supported. Consequently, G is decomposable into a convex combination of Q elementary capacity graphs with $\lambda_1 = \ldots = \lambda_Q = 1/Q$. ■

C. Necessary Condition for Realizability

According to Theorem 3, in order to arrive at a necessary condition for realizability, we can identify cliques in the usage conflict graph U. Note that vertices $\{vw_i\}$ are fully connected and if vw is adjacent to pq in I, then vw_i is adjacent to pq_j, $\forall i, j$. Because of these structural properties, a clique in I can be mapped to a clique in U and vice versa. Thus, we just need to identify cliques in the conflict graph I. Each clique K is a set of links that mutually conflict. Consequently, the following condition is necessary for realizability

$$\sum_{vw \in K} c(vw) \leq 1. \tag{29}$$

Enumerating cliques in a general graph is computationally difficult. However, we may exploit the unique structural properties of the conflict graph due to the interference model.

In [13], Baker, Wieselthier, and Ephremides proposed a simple model for wireless networks, where the only constraint imposed on the nodes is that each node can transmit to or receive from at most one other node at any given time. This model is called "free of secondary interference". As mentioned in Section II-A, the interference model adopted in this paper implies this constraint. Based on this constraint, $|V_0|$ cliques can be identified, each comprising the set of links incident at a node v in the connectivity graph. This results in the following necessary condition

$$\sum_{w \in V_0:\ vw \in E_C} c(vw) + \sum_{w \in V_0:\ wv \in E_C} c(wv) \leq 1, \quad \forall v \in V_0, \tag{30}$$

which has been presented in [2] for computing an upper bound of R_{max} under the free of secondary interference model.

We now present a new method that identifies cliques based on Lemma 1. Recall from Section II-A, when a wireless link ij is active, it exclusively occupies the spatial region $\Omega(ij)$, which is the union of two circles centered at X_i and X_j with radius $\frac{\nu}{2}|X_i - X_j|$. For any spatial location X, we can identity the set of links

$$K(X) = \{ij \,|X \in \Omega(ij)\}. \tag{31}$$

These set of links mutually conflict because the associated spatial regions $\{\Omega(ij)\}$ overlap at point X. Therefore, $K(X)$ is a clique. Hence we have the following necessary condition for realizability.

Theorem 5 (Necessary Condition for Realizability): Let X denote a given spatial location. Under the physical layer model described in Section II-A, a necessary condition for a given capacity graph $G = (V_0, E_C, c)$ to be realizable is

$$\sum_{ij \in K(X)} c(ij) \leq 1, \tag{32}$$

or equivalently

$$\sum_{ij \in E_C} c(ij)\mathbf{I}\left(X \in \Omega(ij)\right) \leq 1, \tag{33}$$

where $\mathbf{I}(\cdot)$ is the indicator function.
Of course, we may check other spatial locations, which may result in different cliques. Note that if we pick X as the location of a node, say X_l, then $K(X_l)$ includes all links that are incident at node l, and possibly others. Therefore, by checking the locations of the nodes, we arrive at a necessary condition that is stronger than (30).

We can integrate both sides of (33) over a give region Ω_0 (or summing both side of (33) over a finite collection of locations). This leads to the following corollary.

Corollary 1: Let Ω_0 denote a given spatial region. Under the physical layer model described in Section II-A, a necessary condition for a given capacity graph $G = (V_0, E_C, c)$ to be realizable is

$$\sum_{ij \in E_C} \int_{X \in \Omega_0} c(ij) \mathbf{I}\left(X \in \Omega(ij)\right) dX \leq \int_{X \in \Omega_0} 1 dX. \tag{34}$$

D. Maximum Scaling of a Capacity Graph

Note that any capacity graph G can be scaled by a sufficiently small number k such that kG is realizable. We can thus define

$$\kappa(G) \equiv \max\left\{k \,|kG \in \mathcal{G}_0\right\}, \tag{35}$$

which is the maximum scaling factor such that the scaled capacity graph is realizable. Lower and upper bounds of $\kappa(G)$ can be constructed from the sufficient and necessary conditions above. For example,

$$\kappa(G) \geq \frac{1}{\max_{vw: vw \in E_C} c(vw) + \sum_{pq:\, pq \in N(vw)} c(pq)}. \tag{36}$$

This lower bound of $\kappa(G)$ holds for general G. For a given G, a better lower bound of $\kappa(G)$ can be found by actually applying the greedy coloring algorithm (Section IV-A) on the usage conflict graph U.

V. Bounding Power Rate Function

To facilitate understanding, we use Figure 5 as a "road map" for this section.

According to Section II-D, given a capacity graph G as the provision of network resources, the maximum rate $R(G)$ that can be achieved can be found by solving a linear program which assigns the multi-commodity flows $\{f^m\}$. A given capacity graph G has an associated power consumption $P(G)$. Thus, the problem of finding the power rate function $P(R)$ turns into one of finding the optimal supported capacity graph, providing a desired rate R at the minimum power consumption.

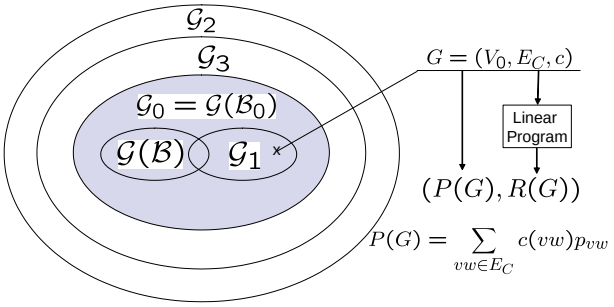

Fig. 5. Relations among different sets of capacity graphs. The entire set of supported capacity graphs is $\mathcal{G}_0 = \mathcal{G}(\mathcal{B}_0)$. Since the number of elementary capacity graphs to be considered can grow exponentially in the number of users, it is computationally impractical to search over $\mathcal{G}_0$. $\mathcal{G}_1 \subseteq \mathcal{G}_0$ is the subset of capacity graphs satisfying the sufficient condition in Theorem 4. $\mathcal{G}(\mathcal{B}) \subseteq \mathcal{G}_0$ is the subset of capacity graphs spanned by a finite number of elementary capacity graphs in $\mathcal{B}$. $\mathcal{G}_2 \supseteq \mathcal{G}_0$ is the set of capacity graphs satisfying the necessary condition in (30). $\mathcal{G}_3 \supseteq \mathcal{G}_0$ is the set of capacity graphs satisfying the necessary condition in Theorem 5. Searching over subsets $\mathcal{G}(\mathcal{B})$ and $\mathcal{G}_1$ yields upper bounds of $P(R)$. Searching over supersets $\mathcal{G}_2$ and $\mathcal{G}_3$ yields lower bounds of $P(R)$.

The physical and link layers of a wireless network can support many different capacity graphs, each being a convex combination of several elementary capacity graphs. Due to the combinatorial nature in arranging concurrent transmissions in the physical layer, there can be an exponential number of elementary capacity graphs to be considered. This renders a full search over the complete set $\mathcal{G}_0$ difficult. In [3], Jain et al showed that finding R_{max} is NP-hard under the interference model characterized by the conflict graph.

The basic idea of the upper-bounding (resp. lower-bounding) approaches to be discussed next is to search over a subset (resp. superset) of $\mathcal{G}_0$, which can be characterized by a finite number of linear constraints. The finite set of linear constraints characterizing the search space of capacity graphs can be combined with the linear constraints characterizing feasible multi-commodity flow assignment, resulting in a joint linear program with power minimization as the objective.

A. Upper-bounding

1) Searching over $\mathcal{G}(\mathcal{B})$: One way to reduce the complexity is to restrict the search space to those composite capacity graphs spanned by a small subset of preselected elementary capacity graphs. With a finite set of elementary capacity graphs $\mathcal{B} \subseteq \mathcal{B}_0$, the convex set of supported capacity graphs becomes

$$\mathcal{G}(\mathcal{B}) = \left\{ G \,\middle|\, G = \sum_k \lambda_k G_k,\ \sum_k \lambda_k \leq 1,\ \lambda_k \geq 0\ \forall k, G_k \in \mathcal{B} \right\}, \tag{37}$$

where the dependence on $\mathcal{B}$ is explicitly shown. Given a finite set of elementary capacity graphs $\mathcal{B}$, the associated convex combination coefficients $\{\lambda_k\}$ can be treated as variables and jointly optimized with the flow variables $\{f^m\}$, resulting in a combined linear program. Such a joint optimization idea was first proposed by Jain et al in [3] to lower bound R_{max}. They suggested a random construction of $\mathcal{B}$. The major drawback with their method is that a more systematic way of efficiently setting $\mathcal{B}$ is lacking. It is unclear how to select a small but "efficient" subset that provide a reasonably good span.

By minimizing $P(G)$ over $\mathcal{G}(\mathcal{B}) \subseteq \mathcal{G}_0$ while providing a rate R, an upper-bound of the power rate function $P(R)$ can be given. However, for a given $\mathcal{B}$, such a linear program may result in a solution where the sum of the flows $F = (V_0, E_C, \phi)$ with $\phi(vw) = \sum_{m=1}^{m} f^m(vw)$, does not match exactly with G. By reducing the provision of resource G to F, which can also be supported, the power can be reduced from $P(G)$ to $P(F)$ while still supporting rate R. Thus, we propose to set the optimization objective as

$$\min \sum_{vw \in E_C} \phi(vw) p_{vw}. \tag{38}$$

The complete linear program is shown in Figure 6. We denote the resulting upper-bound function by $P(R, \mathcal{B})$, where the dependence on $\mathcal{B}$ is explicitly shown.

2) Searching over $\mathcal{G}_1$: Let $\mathcal{G}_1$ denote the set of capacity graphs satisfying the sufficient condition in Theorem 4. Thus, Theorem 4 essentially identifies the subset $\mathcal{G}_1 \subseteq \mathcal{G}_0$, which can be characterized by a set of linear constraints. Searching over $\mathcal{G}_1$ results in the linear program in Figure 7.

The linear program in Figure 7 can be run for different values of R to give an upper-bound function. The linear program in Figure 7 will cease to have a feasible solution for rates larger than a threshold. To find such a threshold, we just need to replace the objective of Figure 7 by

$$\max R.$$

Since $\mathcal{G}_1 \subseteq \mathcal{G}_0$, the threshold is a lower bound to the maximum achievable throughput R_{max}.

B. Lower-bounding

In Section IV-C, we have discussed necessary conditions for realizability of a given capacity graph $G = (V_0, E_C, c)$, which can be expressed as linear constraints in $\{c(vw)\}$. Let $\mathcal{G}_2$ denote the set of capacity graphs satisfying (30). To perform searching over $\mathcal{G}_2$, we just need to replace (51) in Figure 7 by (30).

Similarly, let $\mathcal{G}_3$ denote the set of capacity graphs satisfying $|V_0|$ applications of (33), one for each node's location. With this set of spatial locations checked, $\mathcal{G}_3 \subseteq \mathcal{G}_2$ and hence the resulting lower bound is tighter.

C. The Proposed Bounding Procedure

We explain the proposed bounding procedure as below, which integrates the tools and results developed thus far. To facilitate understanding, we use Figure 10 and Figure 11 in the Simulations section as a concrete example.

1. Run the linear programs that perform searching over $\mathcal{G}_1$ and $\mathcal{G}_3$ while minimizing the power consumption. This gives several power rate pairs, as shown in Figure 10. Each power rate pair (P, R) returned by the linear programs has an associated capacity graphs $\{G\}$, i.e., $(P, R) = (P(G), R(G))$. The points returned by searching over $\mathcal{G}_3$ constitute the proposed lower bound of $P(R)$.
2. For each power rate pair $(P(G), R(G))$ returned by searching over $\mathcal{G}_1$, we apply the greedy coloring procedure described in Section IV-A to actually color the usage conflict graph U. This gives a lower bound of $\kappa(G)$ (Section IV-D), which we denote by κ. Since the scaled capacity graph κG is realizable, power rate pair $(\kappa P(G), \kappa R(G))$ is achievable. Because $\mathcal{G}_1$ is based on a conservative upper bound of $\chi(U)$, $\kappa \geq 1$. In Figure 10, we draw a dashed line that connects each $(P(G), R(G))$ with the scaled version $(\kappa P(G), \kappa R(G))$. It appears in Figure 10 that the points associated with $\mathcal{G}_1$ have been "pushed" upward.
   Apply similar operations to process the power rate pairs returned by searching over $\mathcal{G}_3$. Most points associated with $\mathcal{G}_3$, except those at low rates, appear to be "pulled" downward since they are based on a lower bound of $\chi(U)$. These exceptions occur at small rates where the minimum energy-per-bit is achieved. This is because at a sufficient small rate, the clique constraints are loose. Note that although the points returned by searching over $\mathcal{G}_3$ may not be achievable, the resulting points after the scaling operation are achievable.
3. Compute the convex hull of the set of achievable power rate pairs obtained. The convex hull for the achievable points in Figure 10 is shown in Figure 11.
4. For each collected power rate pair $(P(G^i), R(G^i))$ on the convex hull, we can run the greedy coloring

$$\min \sum_{vw \in E_C} \sum_{m=1}^{M} f^m(vw) p_{vw} \quad \text{subject to:} \tag{39}$$

$$f^m(vw) \geq 0, \quad \forall vw \in E,\ m = 1, \ldots, M \tag{40}$$

$$\sum_{m=1}^{M} f^m(vw) \leq \sum_k \lambda_k c_k(vw), \quad \forall vw \in E_C \tag{41}$$

$$\sum_k \lambda_k \leq 1, \tag{42}$$

$$\lambda_k \geq 0, \quad \forall k \tag{43}$$

$$\sum_{w \in V_0 : vw \in E_C} f^m(vw) - \sum_{w \in V_0 : wv \in E_C} f^m(wv) = 0, \quad \forall v \in V_0 \backslash \{s^m, t^m\},\ m = 1, \ldots, M \tag{44}$$

$$\sum_{w \in V_0 : s^m w \in E_C} f^m(s^m w) - \sum_{w \in V_0 : w s^m \in E_C} f^m(w s^m) = \alpha^m R, \quad m = 1, \ldots, M \tag{45}$$

Fig. 6. A linear program which gives an upper-bound of the power rate function $P(R)$. This essentially performs searching over $\mathcal{G}(\mathcal{B})$.

$$\min \sum_{vw \in E_C} c(vw) p_{vw} \quad \text{subject to:} \tag{46}$$

$$f^m(vw) \geq 0, \quad \forall vw \in E_C,\ m = 1, \ldots, M \tag{47}$$

$$\sum_{m=1}^{M} f^m(vw) \leq c(vw), \quad \forall vw \in E_C, \tag{48}$$

$$\sum_{w \in V_0 : vw \in E} f^m(vw) - \sum_{w \in V_0 : wv \in E} f^m(wv) = 0, \quad \forall v \in V_0 \backslash \{s^m, t^m\},\ m = 1, \ldots, M \tag{49}$$

$$\sum_{w \in V_0 : s^m w \in E} f^m(s^m w) - \sum_{w \in V : w s^m \in E} f^m(w s^m) = \alpha^m R, \quad m = 1, \ldots, M \tag{50}$$

$$c(vw) + \sum_{pq:\ pq \in N(vw)} c(pq) \leq 1, \quad \forall vw \in E_C. \tag{51}$$

Fig. 7. A linear program which gives an upper-bound of the power rate function $P(R)$. This essentially performs searching over $\mathcal{G}_1$.

procedure to decompose G^i into a convex combination of a set of elementary capacity graphs $\{G_k^i, \forall k\}$

$$G^i = \sum_k \lambda_k G_k^i, \quad \sum_k \lambda_k \leq 1,\ \lambda_k > 0. \tag{52}$$

Let $\mathcal{B} = \{G_k^i, \forall k, \forall i\}$, which consists of all elementary capacity graphs that have contributed to the power rate pairs lying on the identified convex hull. With this set of elementary capacity graphs $\mathcal{B}$, we can run the linear program in Figure 6 that performs searching over $\mathcal{G}(\mathcal{B})$. This yields the final upper bound $P(R, \mathcal{B})$. An example can be found in Figure 11.

VI. Simulations

We have conducted simulations on two example community wireless networks. Some simulation parameters are set up as follows. We set $\beta = 3$ (the path loss exponent), $\nu = 1.0$, and $\gamma_1 = 8$. We set p_{max} at a value corresponding to a maximum transmission range of 200m. The power of a link ij, p_{ij}, is normalized with respect to p_{max}. Thus,

$$p_{ij} = \left(\frac{|X_i - X_j|}{200} \right)^3. \tag{53}$$

A. The First Test Configuration

Figure 8(upper) shows the first example community wireless network, in which the locations of the houses

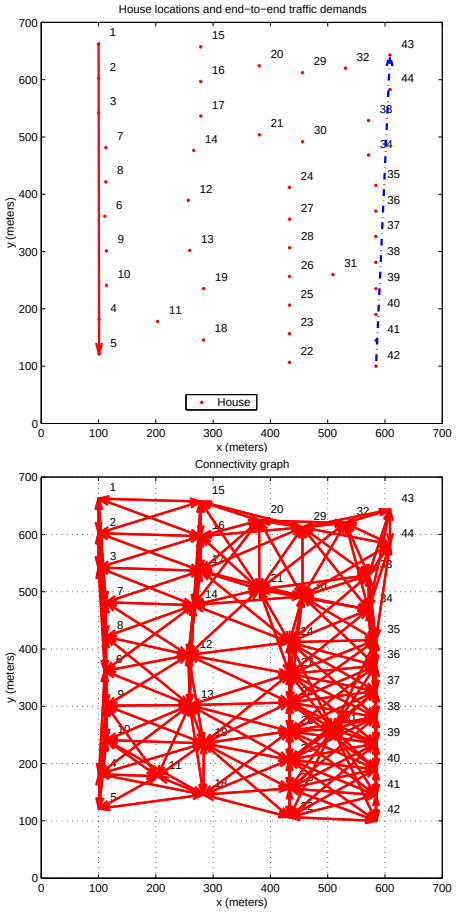

Fig. 8. (upper) The first example community wireless network. (lower) The connectivity graph.

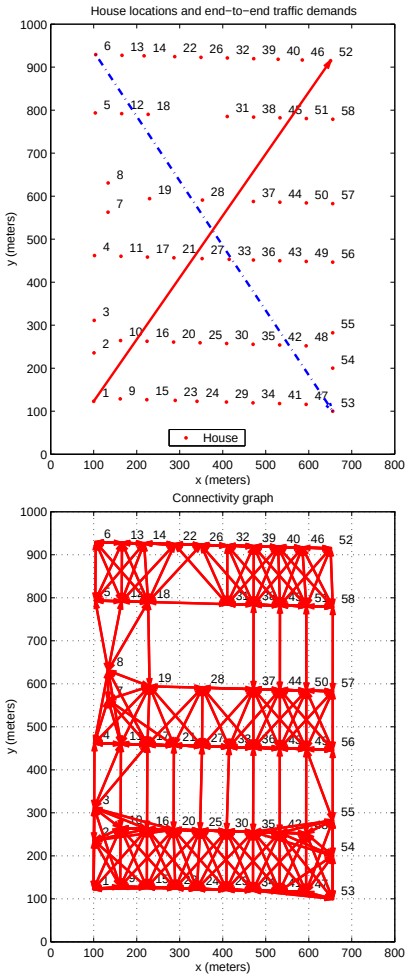

Fig. 9. (upper) The second example community wireless network. (lower) The connectivity graph.

are marked with dots. We consider two unicast sessions $\mathcal{S}_1 = \langle 1, 5, R\rangle$ and $\mathcal{S}_2 = \langle 42, 43, R\rangle$, as illustrated in Figure 8(upper) by two straight lines connecting each source with the associated receiver. Figure 8(lower) shows the connectivity graph, which consists of links with distance less than 200m.

The procedure described in Section V-C is used to compute upper and lower bounds of $P(R)$. We first run linear programs that perform searching over $\mathcal{G}_1$, $\mathcal{G}_2$, $\mathcal{G}_3$, respectively. Recall that $\mathcal{G}_1$ denotes the set of capacity graphs satisfying the sufficient condition in Theorem 4, $\mathcal{G}_2$ denotes the set of capacity graphs satisfying the necessary condition (30), and $\mathcal{G}_3$ denotes the set of capacity graphs satisfying the improved necessary condition in Theorem 5, with the set of spatial check points being the locations of the nodes. The obtained power rate pairs are shown in Figure 10.

It can be observed that the proposed lower-bounding approach, i.e., optimizing over $\mathcal{G}_3$, gives better results than optimizing over $\mathcal{G}_2$. This demonstrates that the necessary condition of Theorem 5 is superior to (30).

As the next step, for each power rate pair $(P(G), R(G))$ returned by searching over $\mathcal{G}_1$ and $\mathcal{G}_3$, we apply the greedy coloring procedure to find a scaling factor κ such that κG is realizable. It can be seen from Figure 10 that the points associated with $\mathcal{G}_1$ have been "pushed" upward, whereas most points associated with $\mathcal{G}_3$, except those achieving the minimum energy-per-bit, have been "pulled" downward. We next compute the convex hull over all achievable points. This is shown in Figure 11. It can be observed that these operations have significantly tightened the upper bound.

Each capacity graph G associated with a point lying on the convex hull is then decomposed with greedy coloring. Taking the union of the useful elementary capacity graphs results in a set $\mathcal{B}$. Finally, searching over $\mathcal{G}(\mathcal{B})$ delivers a better upper bound, since the search space $\mathcal{G}(\mathcal{B})$ contains all capacity graphs that achieve

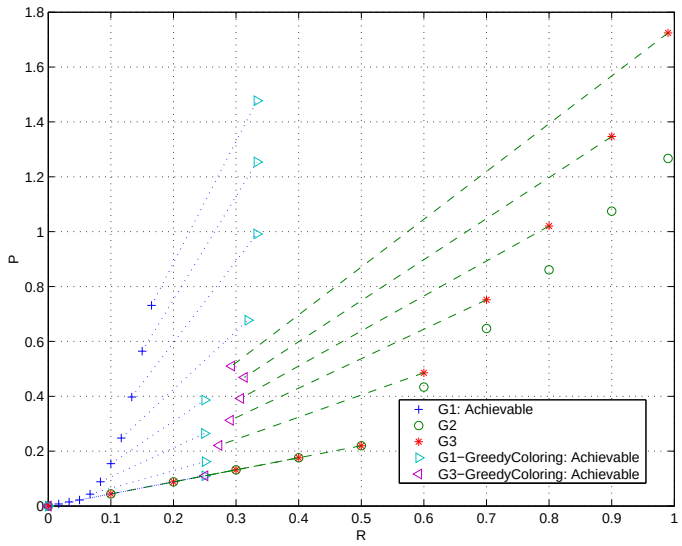

Fig. 10. The power rate pairs returned by searching over $\mathcal{G}_1$, $\mathcal{G}_2$, $\mathcal{G}_3$ and returned by greedy coloring for the first example network.

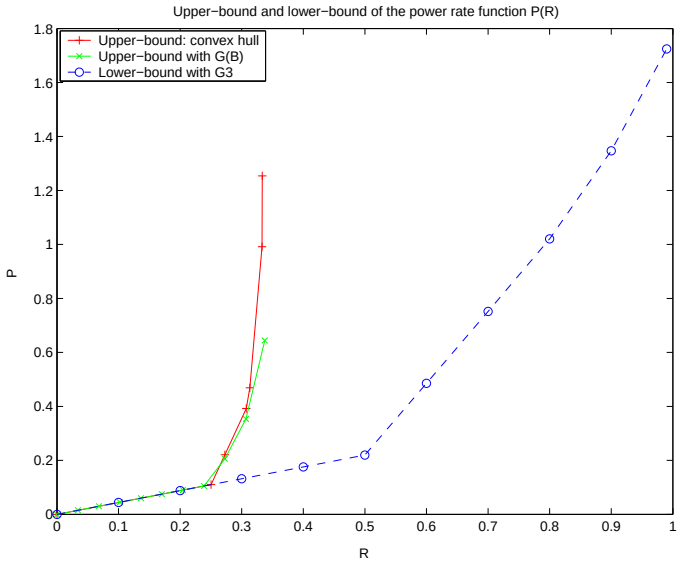

Fig. 11. Two upper bounds and a lower bound of the power rate function for the first example network.

points lying on the convex hull. Comparing the lower bound and the upper bound, it can be concluded that R_{max} lies between 0.33 and 1.0.

Figure 12-15 present the four capacity graphs achieving the last 4 points on the upper bound $P(R, \mathcal{B})$. The provisioned link capacities $\{c(vw)\}$ are shown next to the associated links. As illustrated in Figure 12, when the traffic load is light, each session uses only the minimum energy path. As the traffic load gets heavier in Figure 13, a second route, which is less energy efficient, is used for each session. The connectivity of Figure 14 appears to be similar with that of Figure 13; the difference lies in that more traffic is carried by the less energy-efficient route in Figure 14.

B. The Second Test Configuration

We have also tested the performance over a second example network. The traffic demand and the connectivity graph are given in Figure 9(upper) and Figure 9(lower), respectively. There are 58 houses space roughly in 3 rows. There are two unicast sessions $\mathcal{S}_1 = \langle 1, 52, R \rangle$, $\mathcal{S}_2 = \langle 6, 53, R \rangle$.

Similar as in the first test network, Figure 16 shows the power rate pairs returned by searching over $\mathcal{G}_1$, $\mathcal{G}_2$, $\mathcal{G}_3$ and returned by greedy coloring and Figure 17 gives the final upper and lower bounds. It can be observed that the scaling ("pushing/pulling") of capacity graphs returned by searching over $\mathcal{G}_1$ and $\mathcal{G}_3$ is very useful in producing a better upper bound. In essence, the proposed method of upper-bounding first searches over a large space which coarsely approximate the true solution space $\mathcal{G}_0$. Once the end-to-end traffic demand is mapped into a particular capacity graph G, G can be decomposed at a finer scale with greedy coloring.

For these two test networks, it can be observed that the proposed methods result in very close bounds in the region where both the power and the rate are low. Representative systems operating in this energy-limited regime are sensor networks and UWB systems.

VII. Related Works

Interpreted in the language of the current paper, previous work [2] gave the necessary condition (30) for the realizability of a given capacity graph and proposed searching over $\mathcal{G}_2$ to provide an upper bound of R_{max}.

Previous work [3] by Jain et al introduced the conflict graph and showed that finding R_{max} is NP-hard under the interference model characterized by the conflict graph. Interpreted in the language of the current paper, they proposed to lower bound R_{max} by searching over $\mathcal{G}(\mathcal{B})$ with a random construction of $\mathcal{B}$. The major drawback with their method is that a more systematic way of efficiently setting $\mathcal{B}$ is lacking.

Using the "free of secondary interference" model [13], previous work [7] by Bhatia and Kodialam considered minimizing the total power while providing different rates for a single unicast session. They formulated the

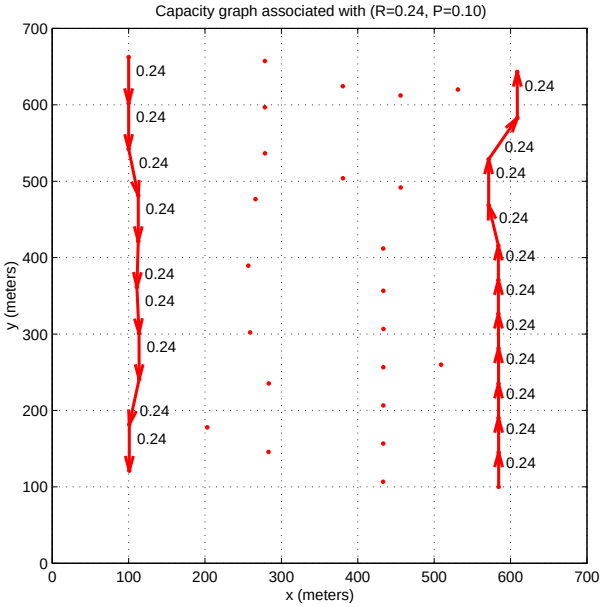

Fig. 12. The capacity graph achieving $(R = 0.24, P = 0.10)$

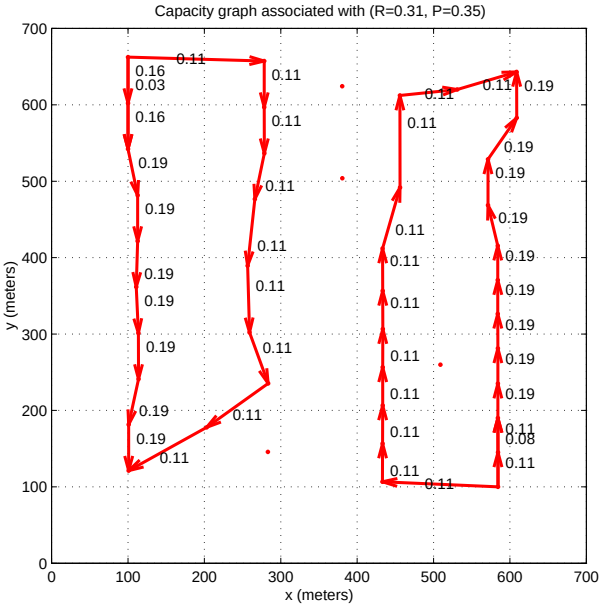

Fig. 14. The capacity graph achieving $(R = 0.31, P = 0.35)$

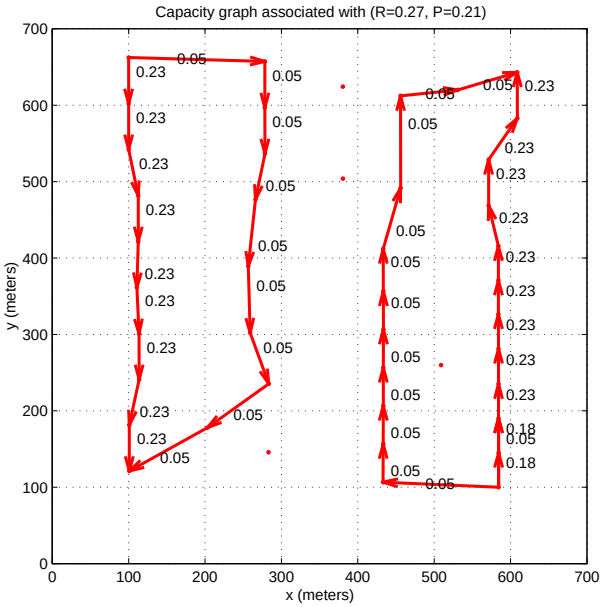

Fig. 13. The capacity graph achieving $(R = 0.27, P = 0.21)$

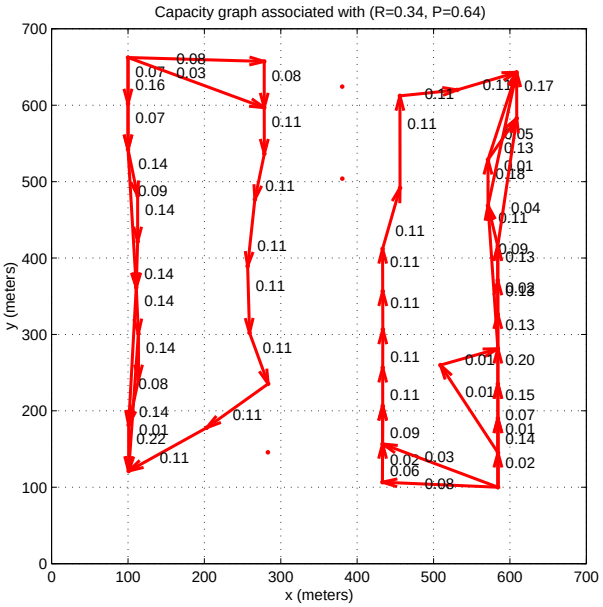

Fig. 15. The capacity graph achieving $(R = 0.34, P = 0.64)$

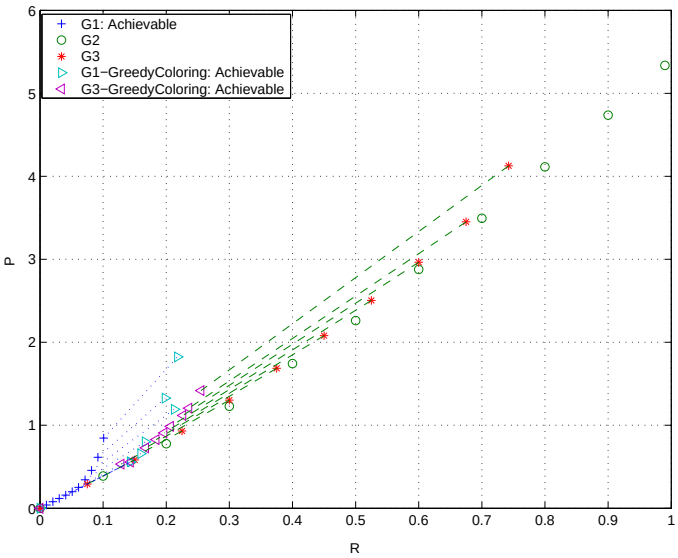

Fig. 16. The power rate pairs returned by searching over $\mathcal{G}_1$, $\mathcal{G}_2$, $\mathcal{G}_3$ and returned by greedy coloring for the second example network.

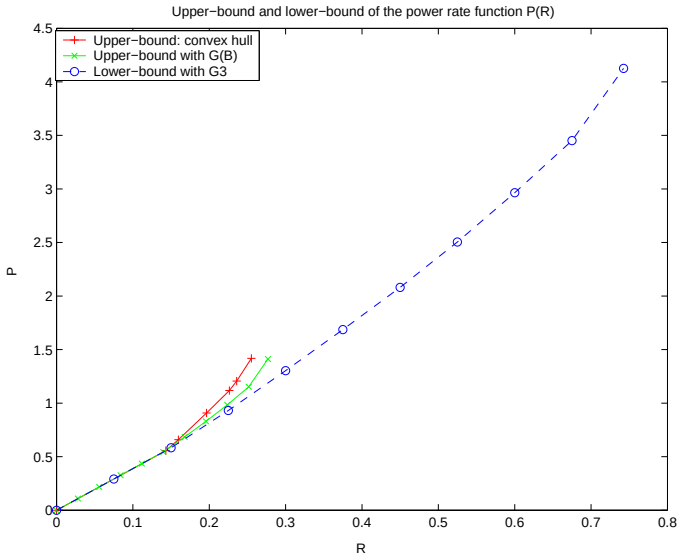

Fig. 17. Two upper bounds and a lower bound of the power rate function for the second example network.

problem as a nonlinear optimization and proposed a polynomial time 3-approximation algorithm.

Previous work [9] by Wu et al presented an iterative optimization that alternates between a linear optimization and heuristic schemes for updating the collection of elementary capacity graphs.

VIII. Conclusions

The power rate function models the tradeoff between rate and energy efficiency for a given wireless network with a given traffic pattern under a layered model of wireless networks. Finding the power rate function involves a cross-layer optimization. A supported capacity graph describes a possible provision of bit-rate resources on the links by the physical and link layers. The entire set of supported capacity graphs of a wireless network $\mathcal{G}_0$ is comprised of convex combinations of elementary capacity graphs. Each supported capacity graph G is capable of providing a maximum rate $R(G)$ and has an associated power consumption $P(G)$. The problem is thus transformed into finding the optimal supported capacity graph associated with each traffic rate R. However, the number of elementary capacity graphs to be considered can grow exponentially, rendering a complete search impractical.

In this paper, we propose a sufficient condition (Theorem 4) and a necessary condition (Theorem 5) for a given capacity graph to be realizable, each of which can be characterized by a polynomial number of linear constraints. The conditions essentially identify a subset $\mathcal{G}_1$ and a superset $\mathcal{G}_3$ of $\mathcal{G}_0$. Searching over $\mathcal{G}_1$ while minimizing power yields an upper bound of $P(R)$. Searching over $\mathcal{G}_3$ while minimizing power yields a lower bound of $P(R)$. We then propose to apply a greedy coloring procedure to fine tune the obtained bounds.

Simulation results on example community mesh networks demonstrate that the proposed bounds are tight in the low power and low rate regime.

In order to focus on the bounding techniques, in this paper, we model the end-to-end traffic demands as multiple unicast sessions. The proposed bounding techniques can be extended to the case with multiple multicast sessions, by replacing multicommodity flow with multicommodity union of flows and taking physical layer broadcast into account.

References

[1] P. Gupta and P. R. Kumar, "The capacity of wireless networks," *IEEE Trans. Inform. Theory*, 46(2), pp. 388-404, Mar. 2000.

[2] M. Kodialam, and T. Nandagopal, "Charactering achievable rates in multi-hop wireless networks: the joint routing and scheduling problem," *ACM MOBICOM*, Sept. 2003.

[3] K. Jain, J. Padhye, V. N. Padmanabhan, L. Qiu, "Impact of interference on multi-hop wireless network performance," *ACM MOBICOM*, Sept. 2003.

[4] S. Singh and M. Woo, "Power-aware routing in mobile ad hoc networks," *Proc. ACM MOBICOM*, 1998.

[5] V. Rodoplu and T. H. Meng, "Minimum energy mobile wireless networks," *IEEE J. Sel. Areas Comm.*, 17(8), Aug. 1999.

[6] A. Ephremides, "Energy concerns in wireless networks," *IEEE Wireless Communications*, pp. 48-59, Aug. 2002.

[7] R. Bhatia and M. Kodialam, “On power efficient communication over multi-hop wireless networks: joint routing, scheduling and power control,” *Proc. IEEE INFOCOM 2004*.
[8] R. L. Cruz and A. V. Santhanam, “Optimal routing, link scheduling and power control in multi-hop wireless networks,” *Proc. IEEE INFOCOM 2003*.
[9] Y. Wu, P. A. Chou, Q. Zhang, K. Jain, W. Zhu, and S.-Y. Kung, “Network planning in wireless ad hoc networks: a cross-layer approach,” submitted to *IEEE J. Selected Areas in Comm.*, Nov. 2003. Accepted for publication.
[10] G. Chartrand and L. Lesniak, *Graphs and Digraphs*, 3rd edition, Chapman and Hall, 1996.
[11] S. Ramanathan, “A unified framework and algorithm for channel assignment in wireless networks,” *Wireless Net.*, Mar. 1999.
[12] R. Diestel, *Graph Theory*, Springer-Verlag, 2000.
[13] D. J. Baker, J. E. Wieselthier, and A. Ephremides, “A distributed algorithm for scheduling the activation links in a self-organizing mobile radio networks,” *IEEE ICC*, pp. 2F6.1-2F6.5, 1982.